

CRITICAL HEIGHT FOR THE DESTABILIZATION OF SOLAR PROMINENCES: STATISTICAL RESULTS FROM *STEREO* OBSERVATIONS

KAI LIU, YUMING WANG, CHENGLONG SHEN¹, AND SHUI WANG

CAS Key Laboratory of Geospace Environment, Department of Geophysics and Planetary Sciences, University of Science & Technology of China, Hefei, Anhui 230026, China

Received 2011 July 26; accepted 2011 September 17; published 2011 December 22

ABSTRACT

At which height is a prominence inclined to be unstable, or where is the most probable critical height for the prominence destabilization? This question was statistically studied based on 362 solar limb prominences well recognized by Solar Limb Prominence Catcher and Tracker from 2007 April to the end of 2009. We found that there are about 71% disrupted prominences (DPs), among which about 42% of them did not erupt successfully and about 89% of them experienced a sudden destabilization process. After a comprehensive analysis of the DPs, we discovered the following: (1) Most DPs become unstable at a height of 0.06–0.14 R_{\odot} from the solar surface, and there are two most probable critical heights at which a prominence is very likely to become unstable, the first one is 0.13 R_{\odot} and the second one is 0.19 R_{\odot} . (2) An upper limit for the erupting velocity of eruptive prominences (EPs) exists, which decreases following a power law with increasing height and mass; accordingly, the kinetic energy of EPs has an upper limit too, which decreases as the critical height increases. (3) Stable prominences are generally longer and heavier than DPs, and not higher than 0.4 R_{\odot} . (4) About 62% of the EPs were associated with coronal mass ejections (CMEs); but there is no difference in apparent properties between EPs associated with CMEs and those that are not.

Key words: catalogs – Sun: corona – Sun: coronal mass ejections (CMEs) – Sun: filaments, prominences

1. INTRODUCTION

Prominences (filaments) are singularities in the corona since they consist of cool (temperature $T \leq 10^4$ K) and dense (electron density 10^9 – 10^{11} cm⁻³) plasma in the hot and diluted coronal medium (Patsourakos & Vial 2002). They are sustained and confined by magnetic field lines above the chromospheres, and exhibit a strong coupling between magnetic forces and thermodynamics (Wiik et al. 1997).

When a prominence ascends with a significant velocity, it is called an eruptive prominence (EP; Pettit 1950). Being one of the earliest known forms of mass ejections from the Sun, EPs started to receive attention in the late 1800s (see Tandberg-Hanssen 1995, chap. 1). Many authors have studied the relationship between EPs and coronal mass ejections (CMEs) and indicate a close association between the two phenomena (e.g., Gilbert et al. 2000; Gopalswamy et al. 2003; Schrijver et al. 2008; Filippov & Koutchmy 2008). House et al. (1981) suggested that the inner core of CMEs is made up of prominence material, which is believed to be the remnants of EPs. So EPs can be treated as a tracer of CMEs (Engvold 2000), and the study of the kinematic evolution of EPs may advance our ability to predict the launch of CMEs.

According to Zirin (1979), prominences are inclined to erupt when their heights exceed 50 Mm. We know that the size and height of a prominence increase with age (Rompolt 1990) and the prominence height characterizes the surrounding magnetic field (Makarov et al. 1992), which is crucial to the stability of prominences. Based on the inverse-polarity model (Kuperus & Raadu 1974), Filippov & Den (2000) deduced that, by assuming the change of magnetic field with height in a power-law function, a quiescent prominence is stable if the power index is less than unity, and will erupt when the power index becomes and exceeds

unity. The magnetic field in the corona at low heights is nearly homogeneous and decreases as the field of a bipole (h^{-3}) at higher heights, thus the equilibrium of a prominence will be unstable when it reaches a certain height. This height is critical for the destabilization of a prominence; thus, we call it critical height. According to Filippov & Den (2000), its value can be calculated by

$$h_c = -\frac{B}{dB/dh|_{h_c}}, \quad (1)$$

where B is the magnetic field strength and h is the height of the prominence. A follow-up study by Filippov & Zagnetko (2008) did show that prominences erupted near the heights calculated by Equation (1).

In this paper, we will re-examine the historical issue statistically by using the EUV 304 Å data from the *STEREO* EUVI instrument. *STEREO* has so far yielded the most complete and uninterrupted observations at an EUV 304 Å wavelength since late 2006. It gave us a chance to study the critical height for prominence destabilization in a statistical way with a large sample. We define a disrupted prominence (DP) as a prominence destabilized during its period of being detected, and a stable prominence (SP) is the prominence elsewhere. In Section 2, we introduce how we chose and classified prominences for our study. The statistical results are given in Section 3. Section 4 is designed for conclusions and discussions.

2. DATA

2.1. Selection of Prominences

Prominences above the solar limb can be clearly detected at an EUV 304 Å wavelength. In our previous work, a system called SLIPCAT (Solar LIMb Prominence CATCHer and Tracker) had been developed to recognize and track solar limb prominences based on only He II 304 Å data observed

¹ Author to whom any correspondence should be addressed:
ymwang@ustc.edu.cn

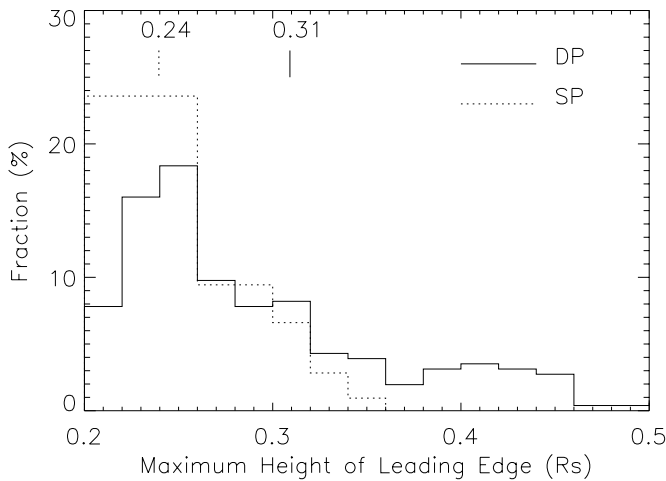


Figure 1. Distribution of the maximum height of leading edges of DPs (solid line) and SPs (dotted line). The short vertical lines with digital numbers mark the average values of histograms.

by SECCHI/EUVI on board *STEREO*. The techniques of region-growing with thresholds and linear discriminant analysis are two major functions applied by SLIPCAT to recognize prominences. SLIPCAT obtained many limb prominences as well as various parameters of each recognized prominence, and a Web-based online catalog has been generated (Wang et al. 2010, hereafter Paper I). Now SLIPCAT has a complete data set for both *STEREO-A* and *STEREO-B* data from 2007 April to 2010 April.²

In this paper, we will use the data set of *STEREO-B* from 2007 April to the end of 2009 for our study. We use *STEREO-B* rather than *STEREO-A* because *STEREO-B* has a larger field of view (FOV) than *STEREO-A*. We do not involve the data after 2010 January, because the solar activity level obviously increased, and the set of calculation parameters used by SLIPCAT is different from that for the *STEREO* data before 2010 (refer to our Web site in footnote 2 for more details).

SLIPCAT extracted 10072 “well-tracked” (see Paper I for the definition of the term) prominences based on SECCHI/EUVI 304 Å data from *STEREO-B* during the period of interest. Further, we narrowed our sample by selecting prominences whose maximum height of the leading edge from the solar

surface was greater than $h = 0.2 R_{\odot}$ (or 140 Mm). We believe that most prominences below $0.2 R_{\odot}$ are not eruptive. A reason for this is that Munro et al. (1979) found that all EPs observed beyond $0.2 R_{\odot}$ were associated with CMEs, which is consistent with Gilbert et al.’s (2000) study, in which it was found that all 18 EPs with a maximum height greater than $0.2 R_{\odot}$ had an associated CME and only one failed to reach $0.2 R_{\odot}$. Moreover, a stronger reason for this is given in Figure 1, which shows the distributions of the maximum height of the leading edges of SPs and DPs (the identification process of SPs and DPs is described in Section 2.2). For SPs, there are more event numbers at a lower height, while for DPs, there is a peak appearing at the middle of the distribution. This indicates that the selection of $0.2 R_{\odot}$ can cover most DPs.

Besides, it should be noted that the prominence height obtained by SLIPCAT is a projected one, and therefore is underestimated. Since a prominence is an extended structure, the underestimation will be even larger for some prominences located at a significant distance away from the limb. For a prominence with its top located 20° away from the limb, its height could be underestimated by $0.06(h+1) R_{\odot}$, which is less than $0.1 R_{\odot}$ in our sample. Hence, we believe that most detected prominences are not too far away from the limb, and therefore the projection effect will not significantly affect our statistical results.

2.2. Classifications of Prominences

Although almost all prominences can be recognized by SLIPCAT, it should be admitted that not all the recognized prominences are real prominences. Some of them are surges, and some are not well recognized but contaminated by noise (Figure 2). Surges have a much different appearance and behavior from a typical prominence. They are relatively narrow and faint, and usually erupt quickly and radially, which means they have a short lifetime. By manually checking EUV 304 Å movies, we removed all surges and noisy prominences from our sample. Meanwhile, all the real prominences were classified into different types according to their dynamic processes when they were detected, which are listed in Table 1.

First, we classified prominences into two main types: SPs and DPs, which have been defined at the end of Section 1. Second, DPs were classified as either EPs or failure eruptive prominences (FPs). We use the definition from Gilbert et al.’s

² <http://space.ustc.edu.cn/dreams/slipcat/>

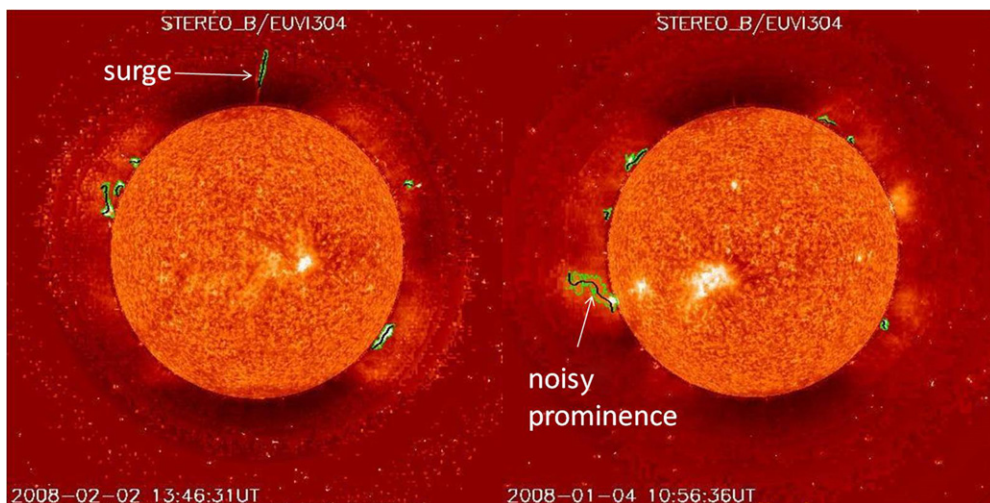


Figure 2. Example showing a surge (left) and a noisy prominence (right).

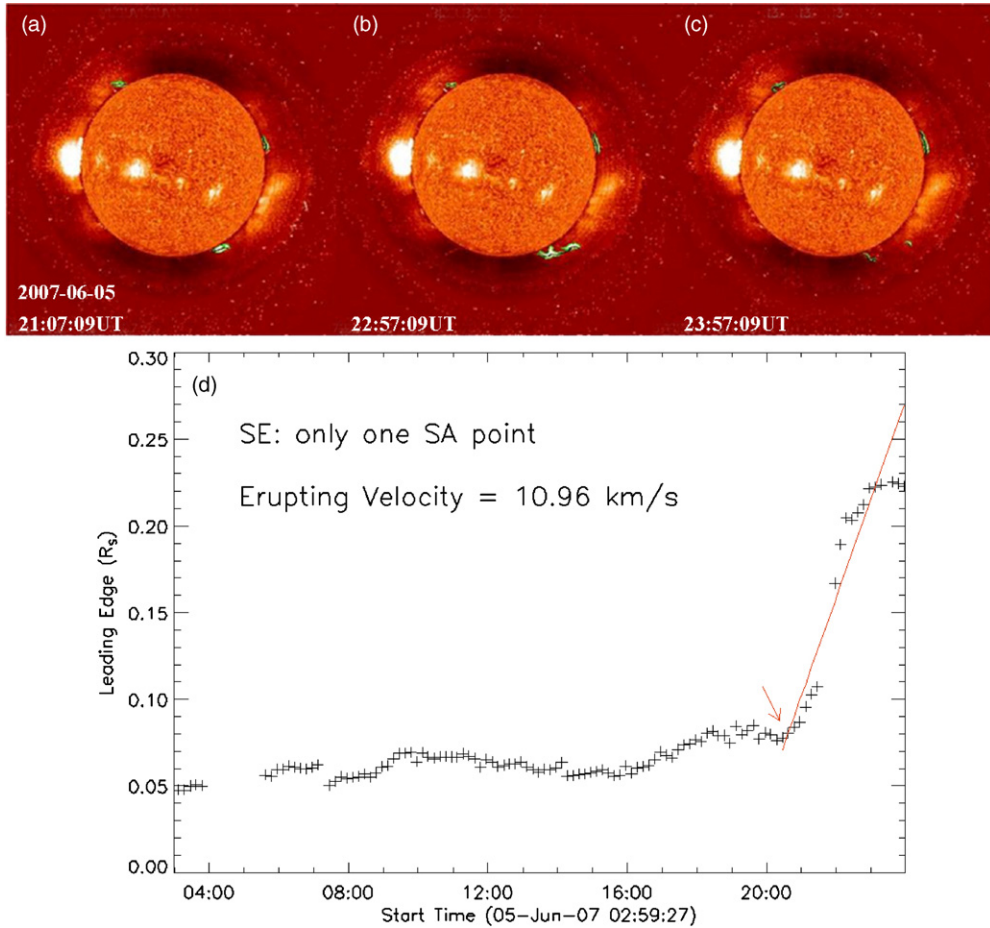


Figure 3. Example of an SE.

Table 1
Classification of Prominences

SPs	DPs			FPs	Total
	EPs		FPs		
	SEs	MEs			
106	70	50	29	107	362
29%	19%	14%	8%	30%	100%

(2000) study to define an EP as a prominence in which all or some of the prominence material appears to escape the solar gravitational field.³ If the ascending prominence material apparently falls back down in the FOV of SECCHI/EUVI ($\leq 1.7 R_{\odot}$ for *STEREO-B*), we call this an FP.

As an EP evolves, its leading edge may gradually rise or may experience one or multiple sudden destabilization (SD) phases. The latter means that there could be one or several points at which the prominence is destabilized. Thus, we further divide EPs into three types. The first type of EP is that with only one SD phase, which we call a single-phase eruption (SE). Figures 3(a)–(c) are three images processed by SLIPCAT showing an SE right before the eruption, during the eruption, and before it faded away around a position angle of about 218° (near the south pole). Figure 3(d) gives the profile of the leading edge of the entire evolution process since 2007 June 5 03:07 UT.

³ Such apparent escaping may be real, but could also possibly be fake due to some thermodynamic processes (see Gilbert et al. 2000 and Paper I). In this paper, we do not distinguish whether an EP actually erupts or is just heated.

It is clear that there is one obvious SD point (denoted by the red arrow), before which the prominence slowly rose with a weak oscillation, and after which it was obviously suddenly accelerated to a significant speed. The SD point indicates the critical height of the destabilization of the prominence and implies a catastrophic process. The erupting speed is estimated to be about 11 km s^{-1} by using a linear fitting.

The second type of EP is more complicated. This type contains EPs with multiple SD phases, which we call a multiple-phase eruption (ME). Figure 4 shows an EP with a position angle around 37° on 2007 June 23, for example. There are three SD points (marked in Figure 4(f) as red arrows) corresponding to three SD phases in this EP's evolution process. The first and third SD phases both indicate a failed eruption, which can be seen from Figures 4(a) and (b) and Figures 4(d) and (e). The second SD phase indicates a successful eruption, which can be seen from Figures 4(b)–(d), and that is the reason we classified this prominence as an EP. We choose the height of the first SD point of the ME as its critical height because that is the point where the prominence loses its stability for the first time. We obtained the eruption speed of this EP by performing a linear fitting to the profile of the successful eruption phase, which is from the second SD point to the point where the escaping material begins to fade away, and the value is about 18 km s^{-1} .

When an EP's leading edge is rising gradually, we call it a gradual eruption (GE), which is the third type of EP classification. We give an example of a GE in Figure 5. Figures 5(a)–(d) demonstrate its appearance from first being detected to fading away around a position angle of 59° . Unlike

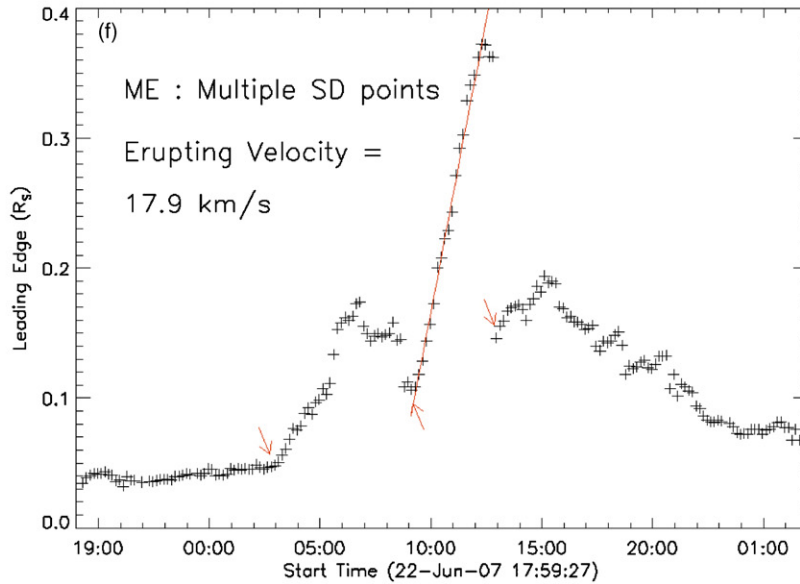
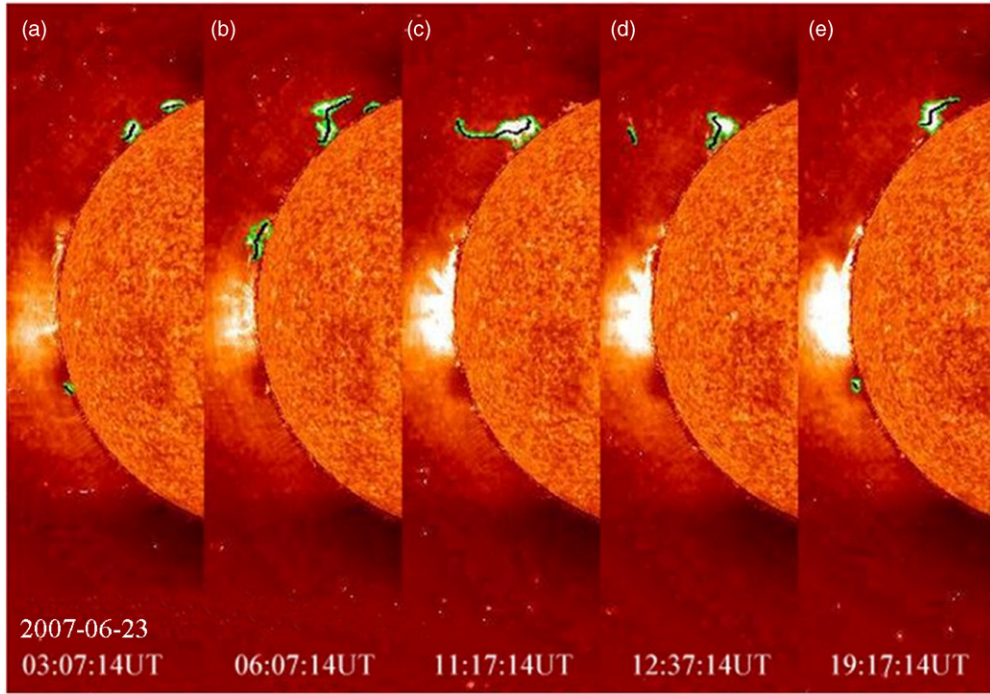


Figure 4. Example of an ME.

the other two types of EPs, a GE does not have an SD point at all, as seen from the evolution profile in Figure 5(e). Thus, we cannot obtain the critical height for the destabilization of this type of EP. The ascending speed of the GE event is about 6 km s^{-1} using a linear fit.

Like EPs, FPs also have one or multiple SD phases, although the erupting materials of FPs fall down eventually according to our data, they also have critical heights for their SD phases. As with EPs, we take the height of the first SD of an FP as its critical height. Thus, in our classification system, SEs, MEs, and FPs have a critical height where they destabilize.

In summary, there are a total of 362 well-recognized prominences with a maximum height of the leading edge above $0.2 R_{\odot}$ detected by *STEREO-B* during 2007 April–2009 December (Table 1). In these events, there are 106 (occupying 29%)

SPs during the period of detection and 256 (occupying 71%) DPs. The latter consists of 107 (42%) FPs and 149 (58%) EPs, and EPs further consist of 70 (47%) SEs, 50 (34%) MEs, and 29 (19%) GEs. We list all the acronyms in the Appendix for reference.

3. RESULTS

3.1. Distribution of Critical Heights

The distribution of the critical heights of EPs (except for GEs) and FPs, which contains 227 data points, is shown in Figure 6. From the histogram, it is found that about 76% of the critical heights fall in the range of $0.06\text{--}0.14 R_{\odot}$ with the mean value at around $0.11 R_{\odot}$. Further, the asterisks connected with lines show the ratio of the number of SEs, MEs, and FPs to the number of all

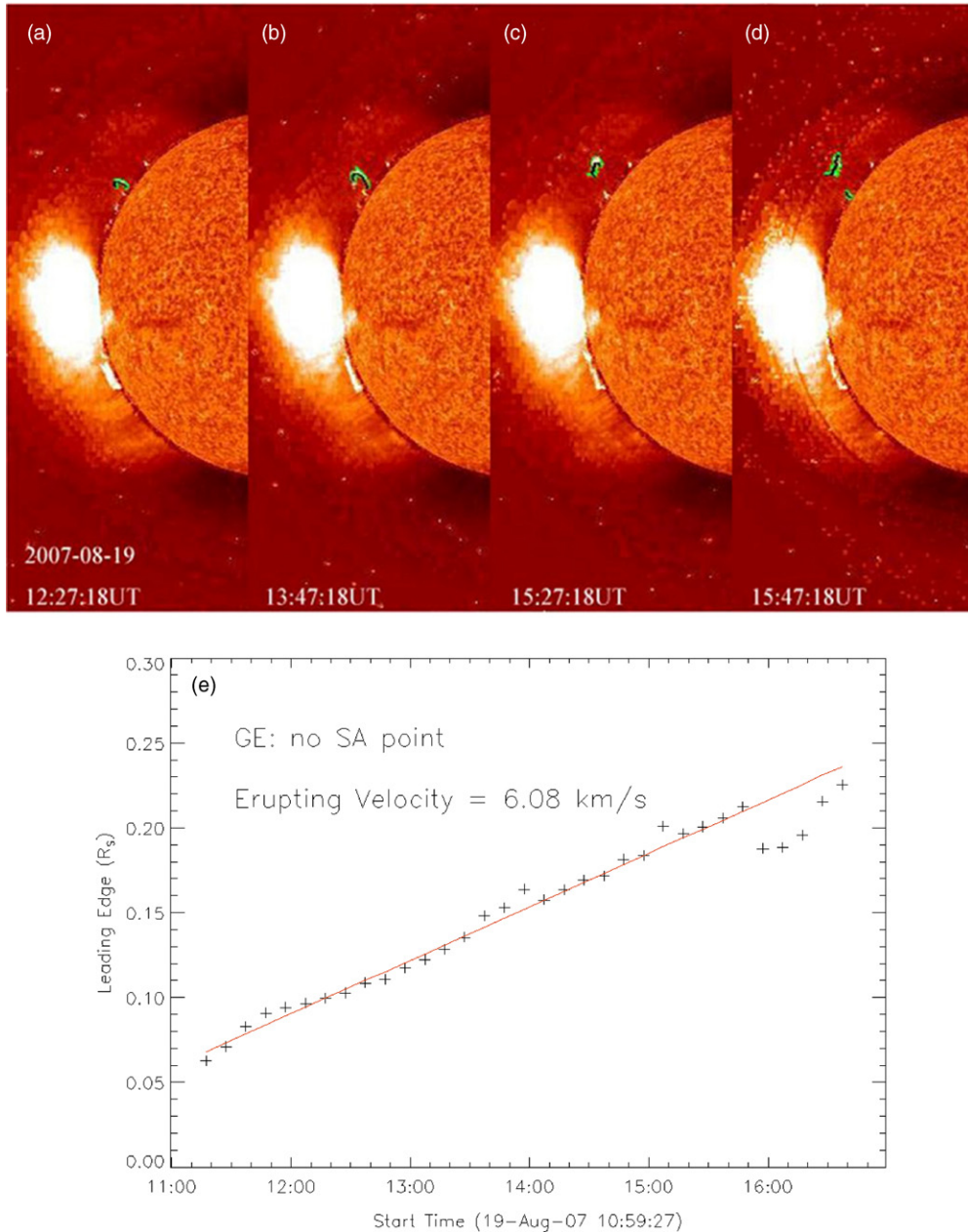


Figure 5. Example of a GE.

prominences recognized by SLIPCAT (for those prominences without a critical height, the maximum height of the leading edge is used). The value of the asterisk actually indicates the probability of a prominence being unstable when it reaches a certain height. The uncertainty is marked by the error bars, which we calculated with the formula $\sigma = [p(1-p)/N]^{1/2}$, where p is the probability and N is the total number of events in the bin. It should be mentioned that the surges and noisy prominences with a maximum height of the leading edge larger than $0.20 R_{\odot}$ are removed, but not for those smaller than $0.20 R_{\odot}$. However, after a quick examination of EUVI movies, we found that most surges and noisy prominences have a maximum leading edge greater than $0.20 R_{\odot}$ and therefore the inclusion of surges and noisy prominences with a maximum leading edge lower than $0.20 R_{\odot}$ will not significantly affect the values of the probability. The probability of distribution above

a height of $0.22 R_{\odot}$ is not reliable, because the event number is small and the uncertainty is significantly large. The small fraction of the events above a height of $0.22 R_{\odot}$ implies that the most probable critical height will not be there. The distribution below a height of $0.22 R_{\odot}$ shows a double-peak feature. The two peaks appear at heights of $0.13 R_{\odot}$ and $0.19 R_{\odot}$, respectively. Since the first one falls in the range of 0.06 – $0.14 R_{\odot}$, in which 76% of critical heights are found, we conclude that $0.13 R_{\odot}$ is the first most likely critical height and $0.19 R_{\odot}$ is the second one.

GEs do not have an SD point despite the fact that they erupt. We examined whether or not their erupting velocities are systematically different from others. This issue is inspected by comparing the distributions of the erupting velocities of GEs and the other two types of EPs (Figure 7). The average velocity of all EPs is about 14 km s^{-1} . It is found that GEs tend to have

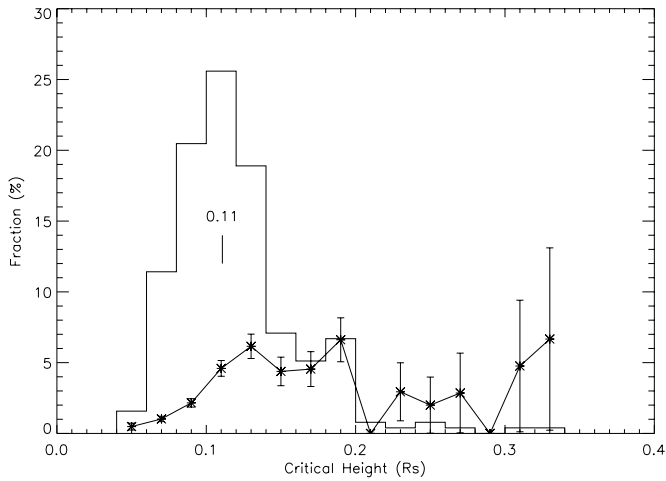


Figure 6. Distribution of critical heights (histogram) and probabilities of prominences becoming unstable at various heights (asterisks connected with lines). See the main text for more details.

a larger erupting velocity. This result is apparently contrary to the usual physical picture that an impulsive eruption (i.e., there is an SD point) should be faster than a GE. One explanation for this is that those fast GEs may have passed through their critical heights before they were recognized by SLIPCAT. It is possible that if most of the GEs were located at a significant distance away from the limb they were not noticed until they had risen or erupted to exceed the limb.

3.2. Erupting Velocity of EPs

The comparison between the erupting velocity of GEs and the other two types of EPs has been presented in the last section. Here we will further investigate the erupting velocities of SEs and MEs and their correlations with critical height and mass. In this study, mass is approximated as the total brightness recorded by *STEREO*/EUVI at a 304 Å wavelength, and in units of digital number (DN). Scattering plots of the erupting velocity versus critical height and the erupting velocity versus mass are shown in Figures 8(a) and (b). It is obvious that the maximum erupting velocity decreases with increasing critical height and mass. This result suggests that, at a certain height or for a certain mass, the kinetic energy an EP could reach or the free magnetic energy accumulated in the prominence-related magnetic system has an upper limit.

In order to obtain the dependencies of the upper limit on the height and mass, we divided the data sample into six bins as indicated by the equally separated vertical dashed lines. The data points with erupting velocity at the top three positions in each bin (marked as plus symbols) are fitted by a function $v = c_0 x^{c_1}$. For Figure 8(a), x is the critical height (h) calculated from the solar surface; for Figure 8(b), x is just the mass represented by the total brightness. The fitting results give the following two equations:

$$v_{\max} = 2.74 h^{-0.99} \text{ (km s}^{-1}\text{)} \quad (2)$$

$$v_{\max} = 1.12 \times 10^5 m^{-0.61} \text{ (km s}^{-1}\text{)} \quad (3)$$

in which h is in units of R_{\odot} and m is in units of DN. Figure 8(c) shows the mass versus the critical height. The darker symbol indicates a larger velocity. Consistent with the above results, the fast erupting prominences are located in the lower left

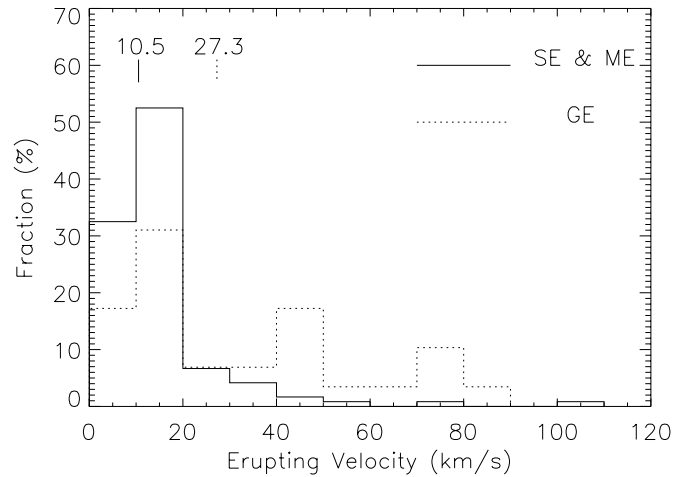


Figure 7. Distribution of EPs' erupting velocity. The vertical lines with DNs indicate the average values.

corner. No obvious correlation between the two parameters is revealed, which indicates that the correlations of the maximum erupting velocity with the critical height and mass are almost independent.

Further, we can derive the upper limit of the kinetic energy of EPs as a function of critical height from the above fitting results as the following equation:

$$E_{\max} \propto m v_{\max}^2 = 2.89 \times 10^8 h^{-0.35} \text{ (DN km}^2 \text{ s}^{-2}\text{)}. \quad (4)$$

The red line in Figure 8(d) presents the equation. Comparing it with the data points in that plot, we can find a weak consistency between them with only four data points exceeding the upper limit.

3.3. EPs versus FPs and DPs versus SPs

Although both EPs (except GEs) and FPs have an SD point, is there crucial difference between the properties of these two types of DPs when they go through an SD point? With this question, we compared their length, area, brightness, and mass at an SD point, and plotted them as histograms in Figure 9. It is shown that there is no obvious difference between the two types, which indicates that one cannot use these properties of a DP at an SD point to decide whether or not it would have a successful eruption.

SPs do not have much change in their properties during their appearances, so we can use the mean values of the length, area, brightness, and mass to present them. We compared these mean values with DPs' properties at an SD point (Figure 10) to check if there is any difference. The histograms in Figure 10 show that SPs generally have a larger length, area, and mass than DPs by a factor of about 1.3. It is reasonable that a large and heavy prominence tends to be stable. This is also consistent with the results obtained in the last section that a prominence with larger mass would have a smaller upper limit of erupting velocity.

3.4. CME Association of EPs

We checked the association of EPs with CMEs by using the same method as Gilbert et al. (2000). First, we determined the position angle and eruption time of an EP of interest. Then we browsed the movies of both coronal observations from COR1 and COR2 on board *STEREO-B* within 2 hr of the eruption time. If there was a CME with a central position angle within

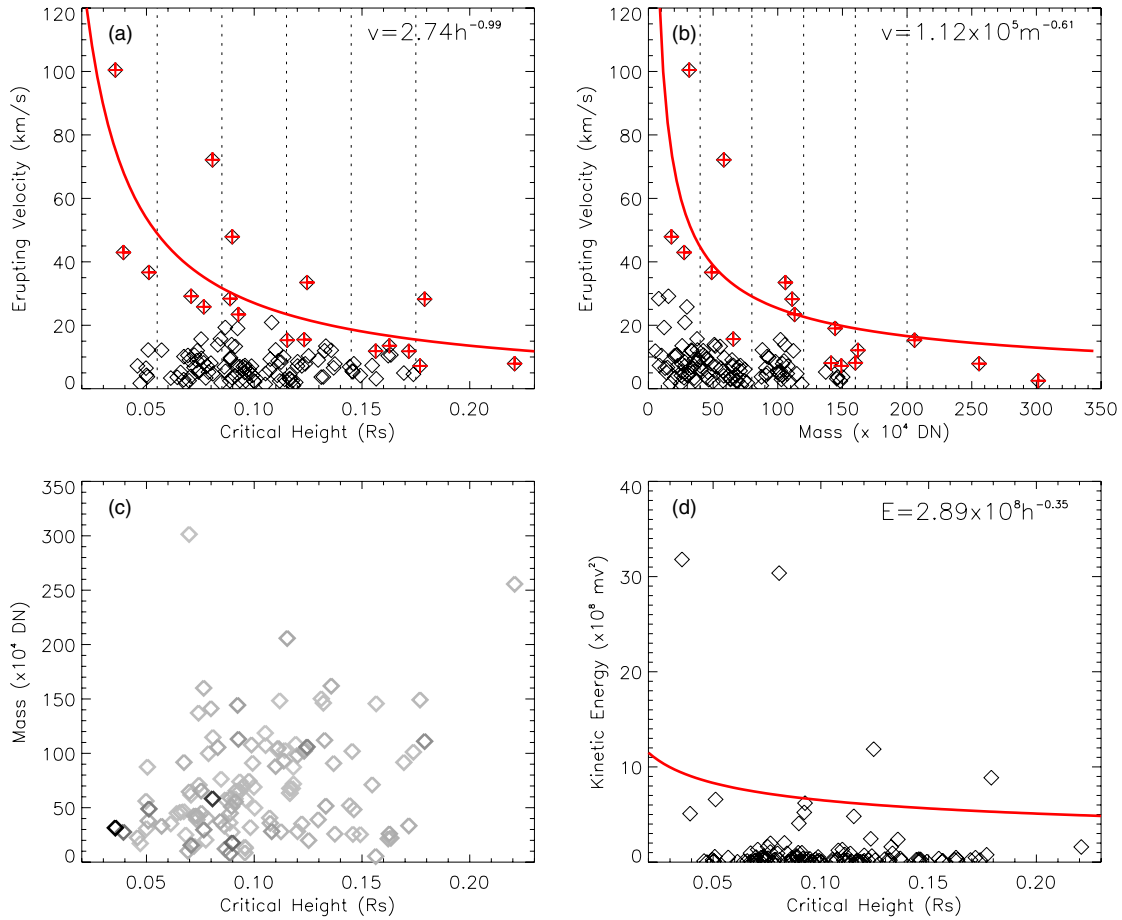


Figure 8. Correlation between (a) erupting velocity and critical height, (b) erupting velocity and mass (represented by total brightness), (c) mass and critical height, and (d) kinetic energy and critical height. In panels (a) and (b), the dashed vertical lines separate data points into six bins, plus symbols mark the data points having the top three erupting velocities in every bin, and the solid line is the fitting curve to them, which is given by the formula in the upper right corner. In panel (c) the darker points have larger erupting velocities. In panel (d) the solid line, given by the formula in the upper right corner, is derived from the fitting functions in panels (a) and (b).

Table 2
Association of EPs with CMEs

Type	CME-assoc./Total	Fraction
SEs	40/70	57%
MEs	35/50	70%
GEs	17/29	59%
Total	92/149	62%

30° of the position angle of the EP in either coronagraph, this EP would be considered to be associated with a CME. The results are summarized in Table 2.

We found that 62% of the EPs are associated with CMEs, and MEs have a relatively higher association rate than the other two types of EPs. The association rate we found is different from that found in previous works, e.g., 94% in Gilbert et al. (2000) and 36% in Yang & Wang (2002). The reason for these differences is mostly due to the data selection. Gilbert et al. (2000) used ground-based observations and picked the prominences that had violent change as their objects. We believe that such a strict selection caused the high association rate. However, Yang & Wang (2002) got a much smaller association rate than others. This is because they treated prominences with transverse motion as EPs too, which are not considered in our

sample. Gopalswamy et al. (2003) obtained an association rate of about 72%. In their work, the data from the Nobeyama Radioheliograph during 1996 January–2001 December were used to identify prominences. Their study covered the period from 1996 January–2001 December, i.e., from solar minimum to maximum, whereas ours is near solar minimum. Thus, their association rate is reasonably larger than ours because CMEs are less frequent in solar minimum than in solar maximum.

We plotted distributions of EPs' critical heights and erupting velocities with (solid line) and without (dotted line) CMEs in Figure 11. They do not show much difference, which suggests that we are probably not able to forecast CMEs' occurrence based only on these properties of EPs.

Figure 11 shows that the average speed of CME-associated EPs is about 14.6 km s^{-1} which is much lower than CME speed, which is typically hundreds of kilometers per second in the outer corona. This divergence implies that prominence materials can be accelerated to considerably high speeds over one or more solar radii. The speeds measured in the EUVI FOV are just initial speeds of prominence eruptions. Also the erupting speeds are much lower than the gravitational escape velocity of $\sim 600 \text{ km s}^{-1}$ at the base of corona, and no obvious deceleration could be found in the velocity profiles. This suggests a continuous driving from released magnetic free energy.

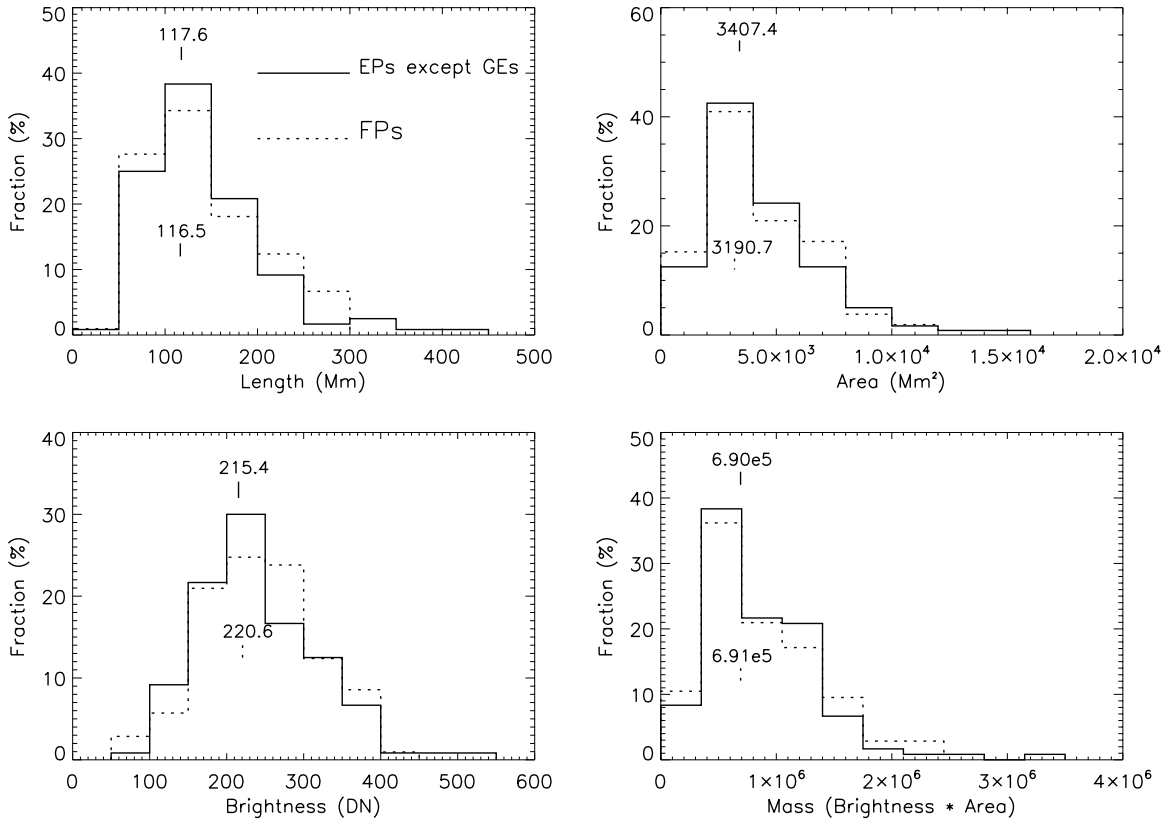


Figure 9. Distributions of the apparent properties of EPs except GEs (solid lines) and of FPs (dotted lines) at an SD point.

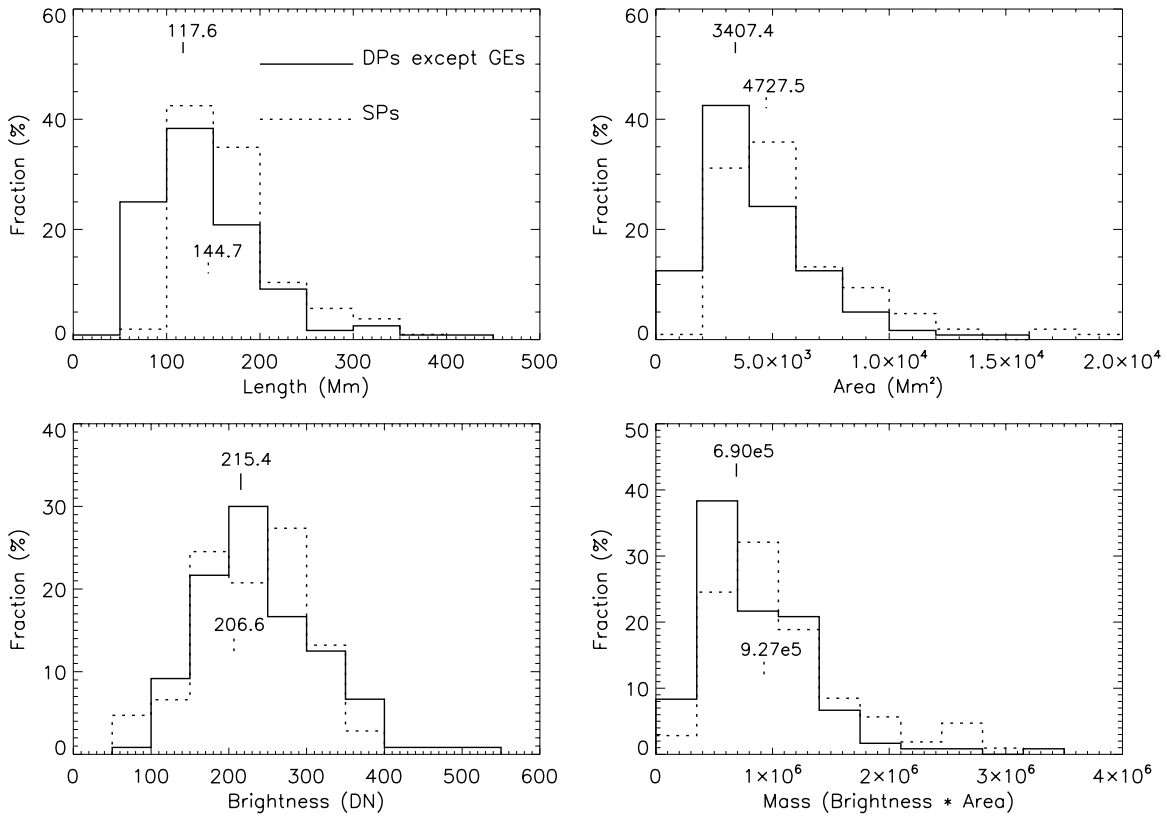


Figure 10. Distributions of the apparent properties of DPUs except GEs at an SD point (solid lines) and the average values of the apparent properties of SPs (dotted lines).

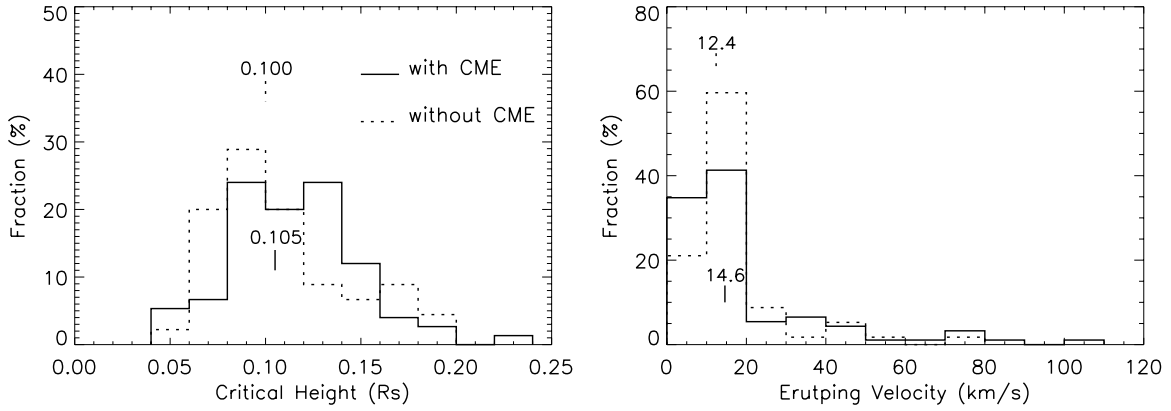


Figure 11. Distributions of critical height (left) and erupting velocity (right) of EPs with (solid lines) and without (dotted lines) CMEs.

4. CONCLUSIONS AND DISCUSSION

All the prominences with a leading edge greater than $0.2 R_{\odot}$ recognized by SLIPCAT during 2007 April–2009 December are investigated. By manually examining the movies, we classified these prominences into various types: SP, DP, EP, FP, SE, ME, and GE. The following statistical results were obtained.

1. About 71% are DPs; about 42% of these DPs did not erupt successfully and about 89% of them experienced an SD process.
2. Most DPs become unstable at the height of $0.06\text{--}0.14 R_{\odot}$. There are two candidates for the most probable critical heights at which a prominence is very likely to become unstable; the first one is $0.13 R_{\odot}$ and the second one is $0.19 R_{\odot}$.
3. An upper limit exists for the erupting velocity of EPs, which decreases with increasing critical height and mass. Inferentially, the upper limit of the kinetic energy of EPs also decreases as critical height increases.
4. There is no difference in apparent properties (length, area, brightness, and mass) between EPs and FPs. However, SPs are generally longer and heavier than DPs by a factor of about 1.3, and no SPs are higher than $0.4 R_{\odot}$.
5. About 62% of EPs were associated with CMEs, but there is no difference in apparent properties between EPs associated with CMEs and those that are not.

According to Equation (1) mentioned in Section 1, we may deduce that prominences embedded in a region with a more rapid decrease in magnetic field strength with height should have a lower critical height. Thus, the first and second most probable critical heights may correspond to two different types of source regions. Prominences can form in an active region or a quiet-Sun region. This may be the reason why two probable critical heights exist. To verify our conjecture, the source regions of DPs and the coronal magnetic field surrounding them must be investigated, which will be pursued in a separate paper.

The corona is dominated by the magnetic field, and therefore the kinetic energy of prominences is converted from magnetic free energy. The anti-correlation of the maximum erupting velocity of EPs with the height suggests that the maximum free energy that could be accumulated in a prominence-related magnetic field system is larger at low altitude than at high altitude. This means that the magnetic free energy decreases as the prominence rises or the surrounding magnetic field structure expands. Approximately, the maximum free energy when the system stays at the critical height can be related to the maximum

kinetic energy of prominences, and is described as

$$E_{\max} = \int \frac{B_f^2}{2\mu} dx^3 \propto \bar{B}_f^2 h^3, \quad (5)$$

where \bar{B}_f is the average magnetic field strength corresponding to the free energy, or approximately the nonpotential component of the magnetic field. In this equation, we implicitly assume that the size of the volume occupied by the magnetic field is proportional to the cubic value of critical height. Combining this with the empirical formula Equation (4), one can easily derive

$$\bar{B}_f \propto h^{-1.7}. \quad (6)$$

This scaling law implies that the average strength of the nonpotential component in a magnetic field structure weakens as the structure rises and expands. However, this result needs to be further justified, because Equation (4) results from hundreds of events and Equation (6) is therefore established from a statistical point of view.

The manual examination of the movies gives us an impression that the entire destabilization process except GEs happened within two data points. One may notice that the cadence of our data is 10 minutes, which means that the catastrophic process of the prominence destabilization is shorter than 10 minutes. A question raised naturally is how quickly such a catastrophic process progresses. To answer this question and study why and how a prominence loses equilibrium, observations with higher spatial and temporal resolutions must be used. Ground-based $H\alpha$ observations may be suitable for such studies, and besides, so far the *Solar Dynamics Observatory* provides the best spaceborne observations that may also be able to support such studies.

The dynamic evolution of prominences can also be related to the large-scale structure in the corona. The coronal cavities were studied by, e.g., Fuller et al. (2008) and Fuller & Gibson (2009), which are generally believed to be flux ropes supporting quiescent prominences. It was found that there were no cavities taller than $0.6 R_{\odot}$. In our study, all SPs were less than $0.4 R_{\odot}$ (Figure 1). The cavity flux rope is kept in equilibrium by two principle forces acting against the natural tendency for the rope to expand outward, namely, the anchored part of the field surrounding the rope and the weight of prominence as well as the coronal helmet, (e.g., see the static model by Low & Hundhausen 1995). Hence, the maximum height for quiescent prominences is physically related to the maximum height of coronal cavities.

We acknowledge the use of data from *STEREO/SECCHI*, and we are also grateful to the developers of SLIPCAT. We thank Dr. B. C. Low for his reading and valuable comments, and the anonymous referee for his/her constructive comments. This research is supported by grants from the 973 key project 2011CB811403, NSFC 41131065, 40904046, 40874075, and 41121003, the CAS 100-talent program, KZCX2-YW-QN511 and startup fund, FANEDD 200530, and the fundamental research funds for the central universities.

APPENDIX

ACRONYMS

AR: Active Region
 CME: Coronal Mass Ejection
 DN: Digital Number
 DP: Disrupted Prominence
 EP: Eruptive Prominence
 EUVI: Extreme Ultraviolet Imager
 FOV: Field Of View
 FP: Failed erupting Prominence
 GE: Gradual Eruption
 ME: Multiple Eruption
 SD: Sudden Destabilization
 SE: Single Eruption
 SLIPCAT: Solar Limb Prominence CAtcher and Tracker
 SP: Stable Prominence
STEREO: Solar TERrestrial Relations Observatory

REFERENCES

- Engvold, O. 2000, International Conference on Solar Eruptive Prominences, http://www-istp.gsfc.nasa.gov/istp/solar_events/ws_html/abstracts.html
- Filippov, B. P., & Den, O. G. 2000, *Astron. Lett.*, **26**, 322
- Filippov, B. P., & Koutchmy, S. 2008, *Ann. Geophys.*, **26**, 3025
- Filippov, B. P., & Zagnetko, A. M. 2008, *J. Atmos. Sol.-Terr. Phys.*, **70**, 614
- Fuller, J., & Gibson, S. E. 2009, *ApJ*, **700**, 1205
- Fuller, J., Gibson, S. E., de Toma, G., & Fan, Y. 2008, *ApJ*, **678**, 515
- Gilbert, H. R., Holzer, T. E., Brukerile, J. T., & Hundhausen, A. J. 2000, *ApJ*, **537**, 503
- Gopalswamy, N., Shimojo, M., Lu, W., et al. 2003, *ApJ*, **586**, 562
- House, L. L., Wagner, W. J., Hildner, E., et al. 1981, *ApJ*, **244**, L117
- Kuperus, M., & Raadu, M. A. 1974, *A&A*, **31**, 189
- Low, B. C., & Hundhausen, J. R. 1995, *ApJ*, **443**, 818
- Makarov, V. I., Tavastsherna, K. S., Davydova, E. I., & Sivaraman, K. R. 1992, *Soln. Dannye, Byull.*, **3**, 90
- Munro, R. H., Gosling, J. T., Hildner, E., et al. 1979, *Sol. Phys.*, **61**, 201
- Patsourakos, S., & Vial, J.-C. 2002, *Sol. Phys.*, **208**, 253
- Pettit, E. 1950, *PASP*, **62**, 144
- Rompolt, B. 1990, *Hvar Obs. Bull.*, **14**, 37
- Schrijver, C. J., Elmore, C., Kliem, B., Török, T., & Trlre, A. M. 2008, *ApJ*, **674**, 586
- Tandberg-Hanssen, E. 1995, *The Nature of Solar Prominences* (Dordrecht: Kluwer)
- Wang, Y., Cao, H., Chen, J., et al. 2010, *ApJ*, **717**, 973
- Wiik, J. E., Schmieder, B., Kucera, T., et al. 1997, *Sol. Phys.*, **175**, 411
- Yang, G., & Wang, Y. 2002, in *Proc. COSPAR Colloq.*, Vol. 14, *Magnetic Activity and Space Environment*, ed. H. N. Wang & R. L. Xu (Boston: Pergamon), 113
- Zirin, H. 1979, in *IAU Colloq. 44, Physics of Solar Prominences* ed. E. Jensen, P. Maltby, & F. Q. Orrall (Cambridge: Cambridge Univ. Press), 193